

Design and Field Evaluation of an Air-Assistance Unit for Spraying Pesticide on a Vertical Crop Canopy

ABSTRACT

Aims: Determination of theoretical requirements of an air assistance unit suitable for coconut palm sprayers

Study Design: The principles of displacement of air volume and terminal velocity for calculating air volume requirement and flow velocity respectively.

Place and Duration of Study: Kelappaji College of Agricultural Engineering and Technology, Kerala Agricultural University, Tavanur Malappuram, Kerala and 3 to 6 months.

Methodology: Based on the theoretical calculation of air volume and flow requirements, an Electric Ducted Fan (EDF) was selected for the air-assistance unit. The EDF offers an effective solution to meet the high air velocity requirements while addressing size concerns. Field trials were conducted to optimise the performance parameters of the EDF, including the air velocity at the fan outlet (10, 15 and 17 m·s⁻¹) and its position relative to the canopy (1, 1.5, and 2 m below the canopy).

Results: The airflow from the EDF effectively reached the top of the canopy, overcoming the challenge of delivering spray droplets to elevated heights in a vertical crop canopy. The adoption of EDF as air assistance unit, addresses the size and weight limitations by providing a higher weight-to-thrust ratio. However, droplet deposition and coverage were found to decrease with increasing spray distance. Operating the sprayer too close to the canopy cause the droplet coalescence, leading to the formation of larger droplets that dripped onto the ground. Over-spraying was more likely when the EDF was positioned too close to the canopy (1 m) at high speed (17 m·s⁻¹), whereas under-spraying occurred when the EDF was placed too far away (2 m). Further studies are recommended to provide a more comprehensive understanding of airflow velocity trajectories within the canopy when spraying in vertical direction against gravity.

Conclusion: Optimal spray deposition and coverage were achieved when the EDF operated at an airflow velocity of 17 m·s⁻¹ and was positioned 1.5 m below the crop canopy.

Keywords: Air-assisted spraying, Droplet deposition, Electric Ducted Fan, Thrust

1. INTRODUCTION

The coconut palm (*Cocos nucifera* L.) cultivation holds substantial role in the agrarian economy of India. Globally, coconuts are cultivated across more than 12 million hectares, with major production hubs in countries like Indonesia, the Philippines, India, Brazil, and Sri Lanka. According to the Food and Agriculture Organization (FAO), the annual global production of coconuts stands at approximately 62 million metric tons in the year 2021, generating substantial revenue and providing livelihoods for millions of smallholder farmers. India is the second-largest producer of coconut, with 14.3 million metric tonnes being produced in 2020. The cultivation of coconut palms faces a significant challenge due to the lack of proper spraying equipment, which adversely impacts yield and overall productivity. One of the major difficulties in managing tall coconut palms is the inability to effectively reach the tree heights during spraying operations. This limitation often results in inadequate pest and disease control, which can severely affect the health and yield of the palms. The traditional method of coconut tree spraying is performed using rocker sprayers, which often leads to pesticide waste and environmental contamination, along with uneven spray patterns that result in poor coverage. Operators face significant health risks from chemical exposure, and excessive pesticide use causes harmful runoff. These issues underscore the need for advanced, efficient, and safer spraying technologies. Among the new advances in spraying technology, air-assisted spraying system and electrostatic spraying system have emerged as promising solutions. Air-assisted spraying technology effectively overcomes the challenges posed by the height of tall coconut palms by using powerful air streams to propel droplets over greater distances, ensuring that the entire canopy, even at the highest points, is uniformly covered. On the other hand, electrostatic spraying systems enhance coverage by charging the spray droplets, enabling them to adhere more uniformly to the palm surfaces. This technology not only improves coverage but also minimizes losses due to drift, making the spraying process more efficient and reducing environmental impact. Together, these innovative technologies represent a significant improvement over traditional methods, addressing the critical challenges of spraying tall coconut palms and leading to healthier crops and higher yields.

Based on the varying canopy characteristics of different plant species and their growth stages, the air flow patterns must be optimized to meet the varying requirements and application efficiency. The air flow generated by the air-assistance unit needs to be sufficiently strong enough to move the leaves within the canopy. A certain air velocity is required for carrying the droplets and impingement of droplets of varying sizes on leaves fluttering in an air stream (Reichardt *et al.*, 1979). According to the principle of air-assisted spraying, the airflow volume of should be equal to the amount of air displaced within the canopy. Which depends on the spatial structure and width of plant canopy (Cross *et al.*, 2003; Gu *et al.*, 2022; Ru *et al.*, 2023; Wang *et al.*, 2023). The air assistance in the spraying process lead to an increased deposition and reduced application rate both in the artificial as well as natural horizontal crop canopy (Gupta *et al.*, 2012). The quantification of air flow velocity required to penetrate the canopy, especially the inner layers was challenging due to the variation in the canopy geometry. In pear orchards, a significant decrease in airflow velocity was observed in the middle and outer layer of the canopy, with a rapid fall occurring within the first 30 cm of the canopy. Beyond this initial section, the reduction in velocity continued but at a slower rate through the 30 to 80 cm range

(Shi *et al.*, 2022). As a result of reduce in velocity, the droplet deposition and coverage may reduce gradually along the range direction (Miao *et al.*, 2023). Comparing to the conventional sprayers, air-assisted electrostatic sprayer has highest deposition and spray coverage in both abaxial and adaxial side because of the air-charge-assistance component (Xue *et al.*, 2023). A simulation study on air velocity distribution with an arc-shaped air outlet found that the arc design improves average wind speed from 14.95 m□s⁻¹ to 18.20 m□s⁻¹ and reduces the proportion of low-speed areas from 20.83% to 0.71%. The best performance is achieved with a rounded corner radius of 50 mm for the air outlet (Jing *et al.*, 2023).

This paper evaluates and optimises the operational parameters of an air-assistance unit for an electrostatic air-assisted sprayer for coconut palms. The electrostatic spray nozzle along with the air assistance unit (spray gun) was mounted on the top end of a 15 m long telescopic pole made of carbon steel. The pump unit, fertilizer tank (5 L capacity), electrical circuit connections for the electrostatic unit and other control knobs are all organised in a backpack-style arrangement. The field evaluation was conducted in the coconut plantation of the Instructional Farm, Kelappaji College of Agricultural Engineering and Technology, Tavanur.

2. MATERIALS AND METHODS

Considering the design requirements of the research, specifically the spraying of coconut palms using a spray gun mounted on top a 15 m long telescopic pole, it is of vital importance that the weight of the blower assembly remains within limits to avoid balancing issues and operator fatigue. Nonetheless, the assembly must generate sufficient thrust force to propel the spray droplets against gravity, ensuring penetration into the canopy and effective targeting of the desired areas.

The spraying unit consists of a backpack structure that houses the battery, pump, pressure gauges, high-voltage circuit for electrostatic spraying, and control units. The backpack unit weighs 8.5 kg, while the spray gun weighs 0.6 kg.

2.1 Theoretical analysis of air flow volume and velocity

The calculation of theoretical demand of air flow volume and air flow velocity of the air-blower system was based on the 'displacement principle of air volume' and 'terminal velocity principle of air flow' respectively (Dai, 2008; Jin *et al.*, 2018; Miao *et al.*, 2023; Wei *et al.*, 2023). The air assistance unit should be capable of transporting the air flow from the fan outlet to the palm canopy and also penetrate through the canopy. According to the principle of displacement of air volume, the displacement area should be the area between the sprayer outlet (width) and boundary of the canopy (length). The volume of air generated by the fan per second due to the movement of sprayer and the constant rotation of fan is equal to the area of the rectangle as shown in Figure 1 (shaded portion). Hence, equation for the required air volume or fan delivery ($Q_{required}$ in m³·s⁻¹) is given as:

$$Q_{required} = v(d + L)(H_1 + H_2)K_1 \quad \text{Equation 1}$$

Where 'd' is the width of spray gun (90 mm), 'v' is the operating speed of sprayer ($0.5 \text{ m}\cdot\text{s}^{-1}$), 'H₁' is the height from the tip of spray gun to the bottom leaf of palm (1.5 m). 'H₂' is the height of canopy (1.5 m), and 'K₁' is the coefficient of airflow attenuation and losses along the way (1.3 to 1.6). By substituting the values in the equation, the required air volume was calculated as $0.867 \text{ m}^3\cdot\text{s}^{-1}$.

According to the terminal velocity principle of air flow, the velocity of air flow must have a minimum level as when it reaches the end of its target range. This ensures the penetration and adhesion of droplets within the crop canopy. The equation for the terminal velocity is as follows:

$$V_2 = K_2 \frac{V_1 d}{L} \quad \text{Equation 2}$$

From the above equation, the velocity required at the discharge outlet is yield as:

$$V_1 = \frac{V_2 L}{K_2 d} \quad \text{Equation 3}$$

Where, 'V₁' is the initial velocity at the outlet in $\text{m}\cdot\text{s}^{-1}$, 'V₂' is the end velocity in $\text{m}\cdot\text{s}^{-1}$. 'L' is the spraying swath in m, and 'K₂' is the coefficient of air resistance and frictional loss along the flow path (1.3 to 1.8). Shi *et al.* (2022) observed that the spraying in orchard canopy (pear) with air assisted sprayers was effective when the terminal air flow velocity was in the range of 2.7 to $3.18 \text{ m}\cdot\text{s}^{-1}$. Miao *et al.* (2023) was taken the terminal air velocity as 2 to $4 \text{ m}\cdot\text{s}^{-1}$ for the design of air-assisted system for high stalk crops. From the literature reviews, the terminal velocity (V₂) was taken as $3.0 \text{ m}\cdot\text{s}^{-1}$. Substituting the values in the equation, V₁ is determined as $14.80 \text{ m}\cdot\text{s}^{-1}$.



Figure 1. Air displacement diagram of the electrostatic sprayer for coconut palms

Hence, from the theoretical analysis, the required air assisted system should be capable of generating an airflow volume of $0.867 \text{ m}^3\cdot\text{s}^{-1}$ and velocity of $14.80 \text{ m}\cdot\text{s}^{-1}$ at the fan outlet. By applying the

equation of continuity, the diameter required for the fan was determined as 27.30 cm, which were found to be significantly larger than the dimensions of the spray gun, and it may also add unnecessary weight to the unit. This is particularly problematic because the narrower top diameter of the telescope must support the weight of the spray gun. To address this issue, a fan unit with a high thrust-to-diameter ratio would be a more appropriate solution, as it would provide the necessary air flow velocity, without contributing excessive weight or requiring a larger diameter.

2.2 Design or selection of air-assistance unit or Electric Ducted Fan (EDF)

Given the outlined considerations, the most appropriate choice for air assistance is to utilize an Electric Ducted Fan (EDF) as the air assistance unit. Because of their high thrust-to-weight ratio and thrust-to-fan diameter ratio, quietness and compactness. In addition, they are easier to construct and operate (Jin *et al.*, 2018; Urban *et al.*, 2023). Ducted fans are capable of generating several fold static thrust for a given diameter when compared to open propeller fans (Urban *et al.*, 2023; Zhao *et al.*, 2022).

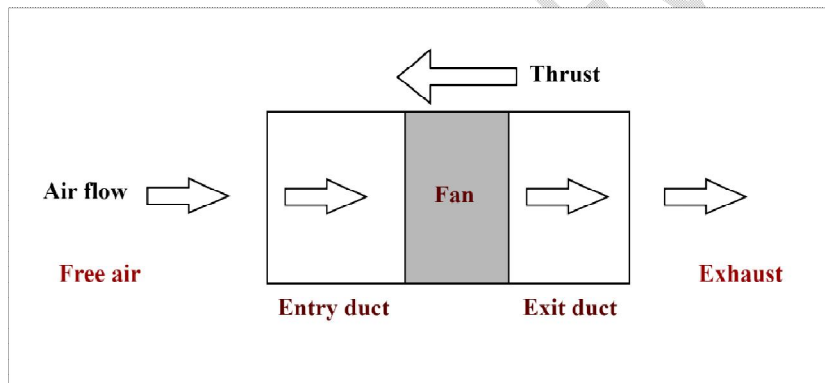


Figure 2. Schematic diagram of an Electric Ducted Fan (EDF)

Electric Ducted Fan (EDF) is basically a small fan or propeller set in an enclosed tube or duct, which is powered by an electric motor as depicted in Figure 2. The design of an EDF is based on the thrust force required in the system. Thrust is the force required to overcome gravity and move an object or provide the desired acceleration, it is generated through the reaction of accelerating a mass of air. (Benson, n.d.; van Oorschot, 2018; Zhang and Barakos, 2020). The thrust developed by an EDF was calculated using the general thrust equation (van Rooij, 2019),

$$Thrust (T) = M dV + \frac{1}{2} \rho (V_e^2 - V_i^2) \times A \quad \text{Equation 4}$$

Where, M is the mass of air being moved or the mass flow rate, in $\text{kg} \cdot \text{s}^{-1}$, dV is the change in the inlet and exit velocity, ρ is the density of air ($1.224 \text{ kg} \cdot \text{m}^{-3}$ at Standard Sea Level), V_i and V_e is the inlet and exit velocity respectively. EDF is primarily employed for aircraft propulsion, particularly for model aircraft and small unmanned aerial vehicles (UAVs). However, under static conditions (zero forward velocity), the EDF functions similarly to its operation in flight. Since, this research is utilizing the EDF

in a stationary position to provide airflow for an air-assisted electrostatic sprayer, it is crucial to understand the performance under static conditions.

Under static operating condition, the forward velocity is zero and the assumption of same inlet and exhaust velocity becomes invalid, as there is a significant difference between the inlet and exit velocities (van Oorschot, 2018; Urban *et al.*, 2023). As the air is sucked into the system from a region of still air, the velocity of inlet air, V_i is infinitesimal. Hence, it was assumed that the change in velocity (dV) closely approximates the exit velocity (V_e) and the power gained system by means of kinetic energy of inlet air was approaching zero i.e. $P_{gain} = 0$ (Sharman, 2011).

$$P_{fan} = P_{loss} - P_{gain} = P_{loss} - 0$$

$$P_{fan} = P_{loss} = \frac{1}{2} M V_e^2 \quad \text{Equation 5}$$

The equation for thrust becomes,

$$T (static) = M V_e + \frac{1}{2} \rho V_e^2 A \quad \text{Equation 6}$$

The power required for the motor to operate fan, P_{motor} , after considering the efficiency of the motor (generally taken as $\cdot 85\%$) and losses in the system due to geometry restrictions and friction in the duct (Ajraoui, 2019; Junaidin and Cahyono, 2019) was calculated as:

$$P_{motor} = \frac{P_{fan}}{0.85} \quad \text{Equation 7}$$

By substituting the values of required airflow volume ($Q_e = Q_{required} = 0.867 \text{ m}^3 \cdot \text{s}^{-1}$), velocity ($V_e = V_1 = 14.80 \text{ m} \cdot \text{s}^{-1}$), and fan diameter in the equations, the minimum required mass flow rate (M) and thrust (T) of the ducted fan was estimated as $1.06 \text{ kg} \cdot \text{s}^{-1}$ and **15.70 N or 1.60kg, respectively**. The power required for the fan was determined as 115 W. Assuming the fan system and motor efficiency as 80 and 85 per cent respectively, the minimum power required for the motor was found to be 170 W. Commercially available brushless motors typically smaller and lighter are capable of achieve higher speed make them suitable for applications demanding high performance and precise control. They are capable of producing substantial thrust even with smaller propellers. Brushless motors paired with electronic speed controllers (ESCs), provide advance speed and direction control.

2.3 Prototype production

The most important design parameter of an EDF is the clearance between the blade tip and inner wall. The other major factors influencing the design are diameter of fan and leading edge, no. of blades, power and kV rating of electric motor. These factors directly influence the structure as well as the performance of the EDF. A prototype of EDF was drawn using the SOLIDWORKS 3D CAD modelling software (SolidWorks Corp., Waltham, MA, USA). Each part of the EDF including blade and outer shell were drawn as separate part in the software and subsequently fabricated using 3D printing technology. The 3D printer (UltiMaker) works on Fused Deposition Modelling (FDM) technology, which

fabricate a model by folding the printing material into individual layers. The printing material was Polylactic acid (PLA), which require a comparatively low printing time. The Figure 3 shows the 3D drawing and the printed prototype of the EDF.

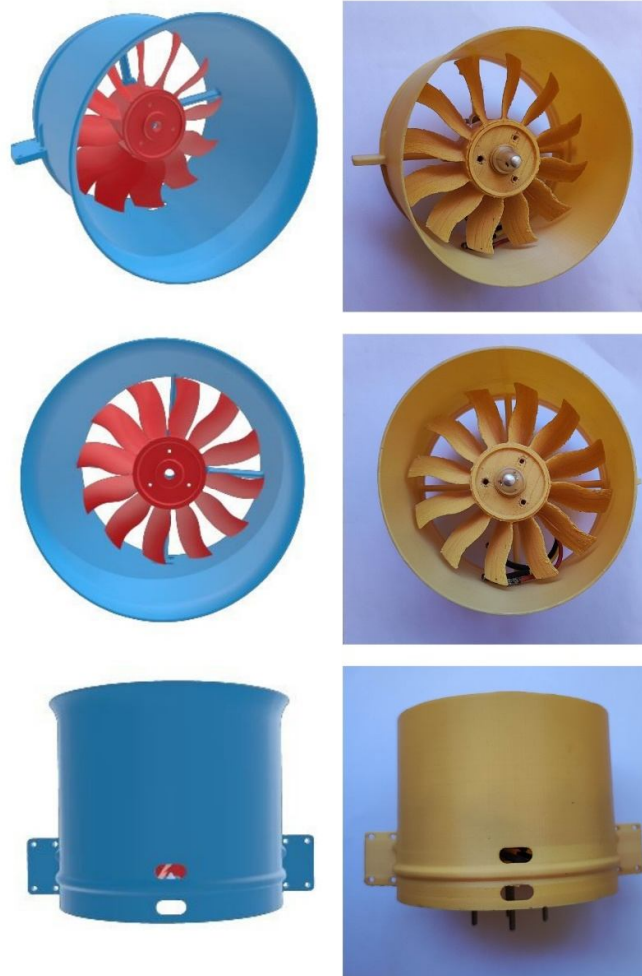


Figure 3. Three-dimensional drawing and 3D printed model of EDF

The fabricated prototype was operated with 1800 kV brushless motor (model: A2212) and powered by a 12 V DC battery (same used for the pump assembly). The observed maximum airflow velocity of the Electro-Driven Fan (EDF) was recorded at $12.20 \text{ m}\cdot\text{s}^{-1}$, which failed to meet the minimum flow velocity requirement. Additionally, when operating the sprayer equipped with the 3D-printed fan, it was noted that the airflow was dispersing laterally rather than maintaining a concentrated, linear trajectory. This dispersion led to a broader and more erratic distribution of spray droplets. These issues are likely attributable to the high surface roughness inherent to the Fused Deposition Modelling (FDM) printing process, coupled with low production tolerance and more clearance between the inner casing walls and the blade tips. The limitations of 3D printing, including its impact on precise fitting and finishing, adversely affect the performance of the prototype. Hence, a commercially available ducted fan with

the same diameter and number of blades were purchased. The details of the purchased EDF were given in the Table 1.

Table 1. Details of 3D printed and Commercially available EDF

Item	3D printed EDF	Commercially available EDF	Design requirements
Fan diameter, mm	70	70	90 mm (Max)
Operating voltage, V	12	12	Suitable
Max. current, A	45	45	Suitable
Rated power, W	540	540	35 (Min)
Thrust at full throttle, kg _f	1.16	2.24	1.60
Motor model	QF2827-1800 kV	QF2827-1800 kV	Suitable
Electronic Speed Controller (ESC) current rating, A	80	80	Suitable

2.4 Field trial

The performance of the developed prototype of air-assisted electrostatic sprayer was evaluated under actual field conditions. The trials were conducted at Instructional Farm of KCAET, Tavanur (10.8412° N, 75.9938° E). Considering the challenges of accessing the upper canopy of coconut palms, the trials were conducted on palms with a maximum height of 7 meters. The palm canopy (leaf bearing portion) was divided into three sections, bottom (B), Middle (M) and Top (T) for the measurements. The sprayer was operated at $5 \text{ kg} \cdot \text{cm}^{-2}$ and discharge of $7 \text{ L} \cdot \text{h}^{-1}$. During the spraying the operator was moved around the coconut palm in a uniform speed.

The blower was operated at three different speeds, corresponding to air flow velocities labelled as 10, 15 and $17 \text{ m} \cdot \text{s}^{-1}$, with the **Water Sensitive Papers (WSPs)** placed on the bottom, middle, and top leaves. The Electric Ducted Fan (EDF) was positioned at heights of 1, 1.5, and 2 meters below the canopy, measured from the position of the lowest leaf. During the field trials, it was observed that spraying at $10 \text{ m} \cdot \text{s}^{-1}$ air velocity was ineffective in delivering droplets to the canopy, as the air velocity was insufficient to overcome the downward pull of gravity. Consequently, subsequent field trials were conducted using air outlet velocities of 15 and $17 \text{ m} \cdot \text{s}^{-1}$.

The droplet deposition and coverage were determined using the water-sensitive papers (WSP) of size $26 \times 76 \text{ mm}$ (Aadhaar Green Solutions, Delhi). The WSPs were (fixed with clip) positioned at the abaxial and adaxial side of the top (T), middle (M) and bottom (B) leaves. The sprayer was operated initially for 60 and 30 seconds prior to the field trials and observed that dripping from the bottom leaves while spraying for 60 seconds and hence the field trials were conducted with spraying for 30 seconds. The sprayer was operated for 30 seconds and waited some time for the water sensitive papers to dry. The WSPs are collected carefully and then transferred to zip lock covers and stored

under shade until processed. Each WSPs are then scanned at 600 dpi resolution using Epson M2170 scanner.

3. RESULTS AND DISCUSSION

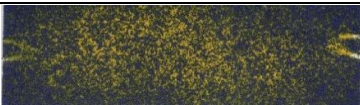


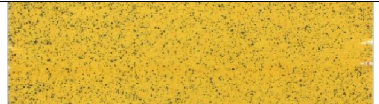


The design or selection of suitable air-assistance unit were done based on the theoretical requirement of air flow volume and air flow velocity to cover 1 m spraying swath of the developed nozzle. From these calculations, the thrust and power requirement of the fan unit have been derived, which ensures that the fan unit aligns the specified parameters.

3.1 Possibility of overspray and under spray

When the sprayer was operated with the EDF positioned 1 meter below the canopy, the water-sensitive papers (WSPs) in the bottom layers mostly turned blue, indicating a saturated spray with a coverage percentage of approximately 50 to 60 percent for both 15 and 17 m·s⁻¹ air velocities. In the middle layers, the WSPs showed signs of overspray, with coverage percentages ranging from 30-40%. Whereas, adequate spray patterns were observed in the upper middle layers as shown in Table 2.

When the sprayer was operated from a position 1.5 meters below the canopy, adequate spray patterns were achieved across all layers with 17 m·s⁻¹ air velocity. However, for 15 m·s⁻¹ air velocity, adequate patterns were observed only in the bottom and middle layers. The upper middle layer exhibited under spray or insufficient spray patterns at 15 m·s⁻¹ air velocity. When the sprayer was operated from 2 meters below the canopy, middle and bottom layer showed under spray pattern for both 15 and 17 m·s⁻¹. Whereas bottom layer was sufficiently exposed to the spray cloud when operated with 17 m·s⁻¹ air velocity.

Table 2. Samples of Water Sensitive Papers collected at different operating positions of the sprayer

Sprayer operated from 1 m distance		
Sprayer operated from 1.5 m distance		
Sprayer operated from 2 m distance		

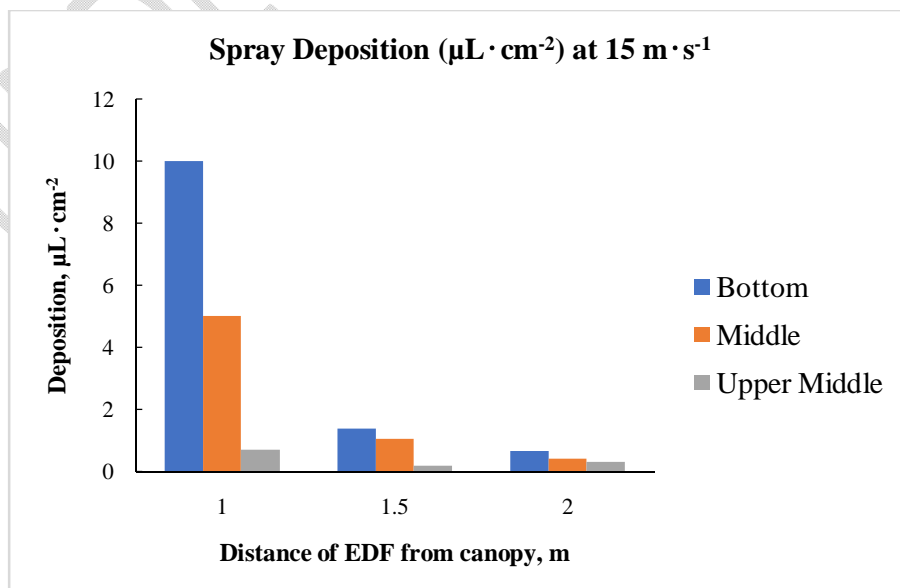
Adequate spray (30%) at
bottom layer

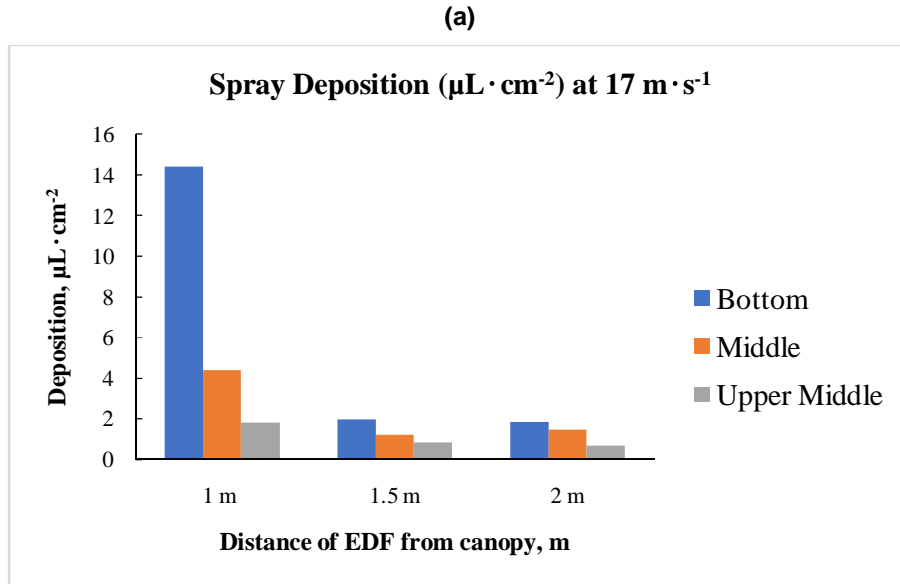
Under spray (6%) at middle
layer

3.2 Distribution of droplet deposition

The droplet deposition at two operating velocities is shown in Figure 4 **Error! Reference source not found.** There was a clear trend of decreasing the droplet deposition along the direction of range for all the air outlet velocities. Furthermore, the deposition was decreasing with the lowering the position of EDF. When spraying was conducted from a point 1.5 m below the canopy, the resulting deposition ranged from 0.8 to 1.9 $\mu\text{g}\cdot\text{L}^{-1}$ at both operating speeds, which achieved the optimal spray deposition. In contrast, when the EDF was positioned 1 meter below the canopy, **the deposition increased by 4 to 10 times in bottom and middle canopy sections compared to that at the 1.5 m position.** Further lowering the EDF to 2 meters resulted in a decrease in deposition at 15 $\text{m}\cdot\text{s}^{-1}$. Whereas at 17 $\text{m}\cdot\text{s}^{-1}$, similar deposition levels as in 1.5 m was observed.

In all operating air velocities and EDF positions, the leaves located in the lower layers of the canopy exhibit higher deposition rates, as they are more directly exposed to the spray charge. As the spray cloud penetrates through the canopy, the middle and upper middle layers receive exposure to the droplets, but to a lesser extent. With the EDF operating at a position of 1.5 m, the average deposition in the middle layer was measured as 1.232 and 1.045 $\mu\text{g}\cdot\text{L}^{-1}$ for air velocities 15 and 17 $\text{m}\cdot\text{s}^{-1}$, respectively. Whereas the upper middle layer received less exposure to the droplet charge under same operating conditions. This reduced deposition is due to the longer distance the droplets must travel through the canopy, principally against gravity. The average deposition observed in the upper middle layers at 1.5 m operating position of EDF was 0.884 and 0.201 $\mu\text{g}\cdot\text{L}^{-1}$ respectively for 15 and 17 $\text{m}\cdot\text{s}^{-1}$ air velocities. **Statistical analysis at 95 per cent confidence level (Table 3) shows that the blower speed and the combination of EDF speed with position has gas no significant effect on the spray deposition, whereas the EDF position has a significant effect.**



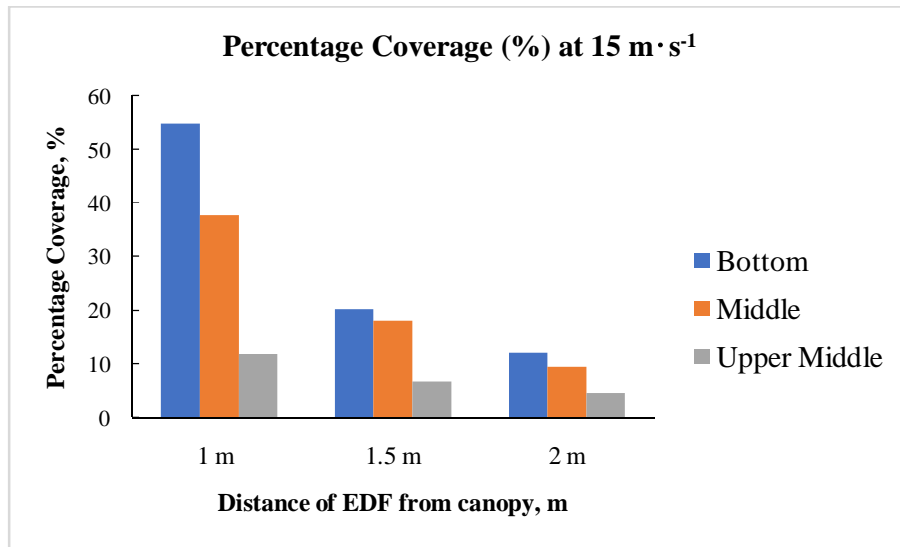


(b)

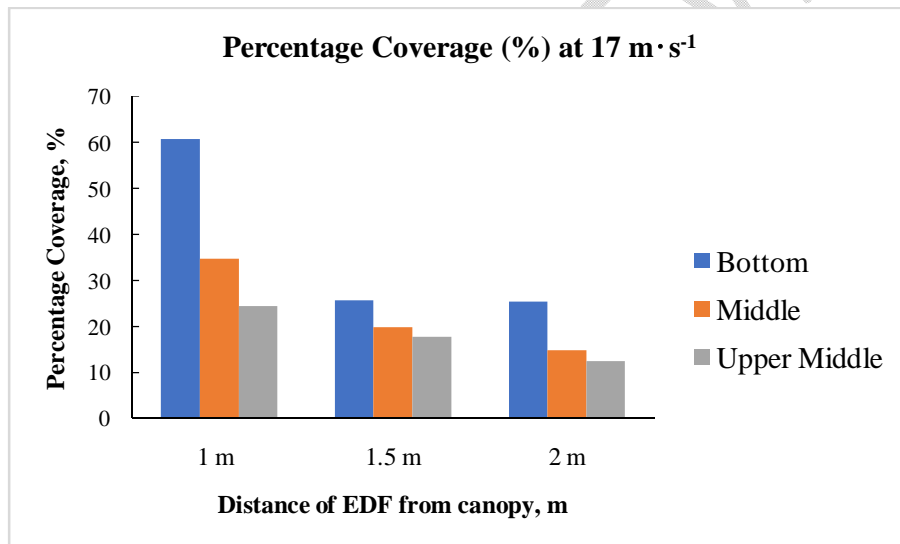
Figure 4. Spray Deposition at different operating conditions of EDF (a) 15 m · s⁻¹ air flow velocity (b) 17 m · s⁻¹ air flow velocity.

3.3 Distribution of droplet coverage

Figure 5 shows the droplet coverage in each layer at different operating position and air flow velocity. There was clear trend of decrease in the droplet coverage with lowering the operating position and increase in the range of spraying. The bottom layers have percentage coverage in the range of 50 to 60 percent, which were considered as over sprayed as discussed before. The middle layer was observed with droplet coverage in an optimum range for almost all the operating conditions except at 2 m position with 15 m · s⁻¹ air velocity. However, the upper middle layer was most likely with minimum coverage for all operating condition except at 1.5 m position and BS3 air velocity. An optimum spray coverage in the range of 17 to 25 per cent was observed in all layers of the canopy when the operating conditions 1.5 m position and 17 m · s⁻¹ air velocity. From the statistical analysis (Table 3), it was concluded that both the EDF operating speed and position has significant effect on the droplet coverage at 95 per cent confidence level.



(a)



(b)

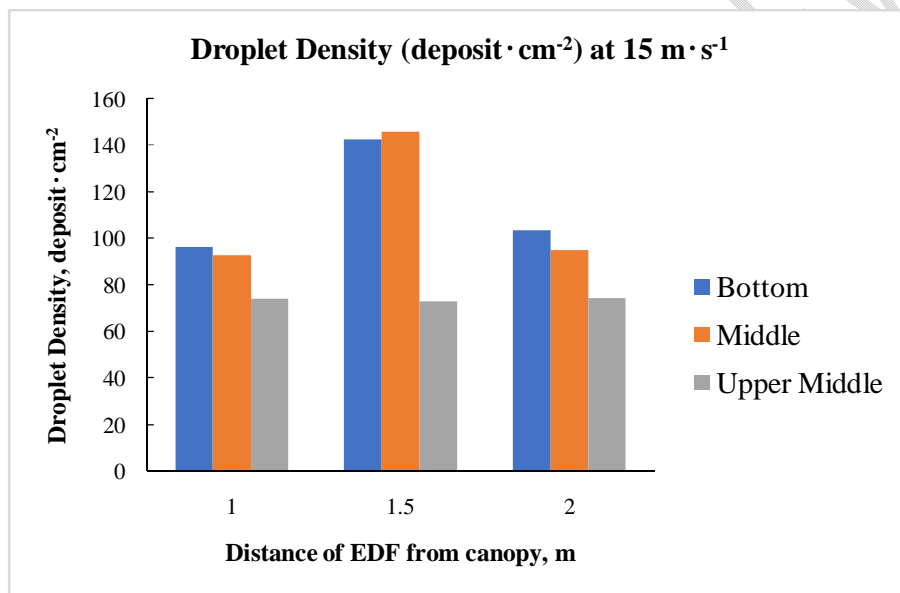
Figure 5. Percentage coverage of spray droplets at different operating conditions of EDF (a) 15 m·s⁻¹ air flow velocity (b) 17 m·s⁻¹ air flow velocity.

3.4 Droplet density

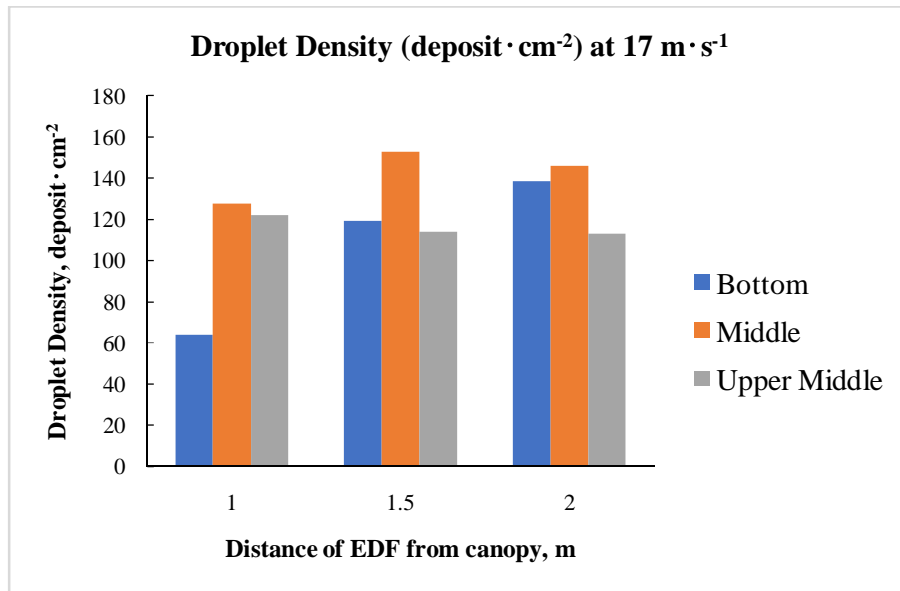
The droplets per unit area on WSP helps in determining the effectiveness and uniformity of spray distribution. The droplet density for different operating condition was shown in the Figure 6. It was observed that, the droplet density of the middle layer has the maximum droplet density irrespective of the operating conditions. The bottom layer of the canopy has more droplet density compared to the upper middle layer for all the operating conditions. However, droplet density at bottom layer at 1 m operating position and 17 m·s⁻¹ air flow velocity contradicts this trend, which has the minimum value

of droplet density ($63.8 \text{ deposit} \cdot \text{cm}^{-2}$). The highest value of droplet density was observed as $152.76 \text{ deposit} \cdot \text{cm}^{-2}$ in the middle layer when the sprayer was operated at 1.5 m position and EDF was operated at $17 \text{ m} \cdot \text{s}^{-1}$ air velocity.

The middle layer was moderately exposed to the droplet spectrum for all the operating conditions and hence, they have the highest droplet density compared to the other layers. But the bottom layers are directly exposed to the spectrum, which may lead to coalescence of droplets after they get deposited for the canopy. The aggregation of droplet leads to the formation of bigger droplets. The bigger droplets cover larger area and which in turn reduces the droplet deposit per unit area. As the sprayer operated very close to the canopy with higher air outlet velocities of EDF, the chances of coalescence of droplets increases, leads to a minimum value of droplet density.



(a)



(b)

Figure 6. Droplet density at different operating conditions of EDF (a) 15 m · s⁻¹ air flow velocity (b) 17 m · s⁻¹ air flow velocity.

As the range of spraying increases, the droplet spectrum has to travel long distances to reach the target. The long travel path increases the chance of losses of spray droplets through evaporation as well as drift. This will result in reduced deposit per unit area in the upper middle layers for all the operating conditions. The statistical analysis shows that the speed of EDF has a significant effect on the droplet density, however, position of the EDF does not have any significant effect at 95 per cent confidence level.

Table 3. Significant effect of the blower speed and EDF position on percentage coverage, droplet density, and spray deposition at 95.0% confidence level. Significant level: NS: P-Value >0.05; S: P-Value ≤0.05.

Main effects	Percentage coverage		Droplet density		Spray deposition	
	P value	Statistical significance level	P value	Statistical significance level	P value	Statistical significance level
EDF speed	0.032	S	0.017	S	0.247	NS
EDF position	0.018	NS	0.979	S	0.053	S
Blower speed × EDF position	0.882	NS	0.123	NS	0.734	NS

4. CONCLUSION

The field trials on the air-assistance unit (EDF) of an electrostatic sprayer for coconut palm showed that the air flow could reach up to the top end of the canopy. Thus, the difficulty in reaching the spray droplets in heights while spraying in a vertical crop canopy can be addressed with the air-assistance spraying. Moreover, the size and weight limitations can be solved us by adopting fan or blower units with more weight to thrust ratio as EDF.

The droplet deposition as well as droplet coverage were decreasing along the range of the spray. When the sprayer was operated near to the canopy, coalescence of the spray droplet may lead to the formation of larger droplets, which in turn caused dripping of the spray solution to the earth. The chances of over spraying were predominantly occurred when the EDF was positioned closer to the canopy (1 m) with the higher speed and under spray patterns were noted when the EDF placed too far away (2 m) from the canopy. An optimum spray deposition and coverage were observed when the EDF operated at an air flow velocity of $17 \text{ m}\cdot\text{s}^{-1}$ and at 1.5 m below the crop canopy. Further studies on this topic may help to give more comprehensive understanding of the flow velocity trajectories within the vertical canopy.

Disclaimer (Artificial intelligence)

Option 1:

Author(s) hereby declare that NO generative AI technologies such as Large Language Models (ChatGPT, COPILOT, etc.) and text-to-image generators have been used during the writing or editing of this manuscript.

Option 2:

Author(s) hereby declare that generative AI technologies such as Large Language Models, etc. have been used during the writing or editing of manuscripts. This explanation will include the name, version, model, and source of the generative AI technology and as well as all input prompts provided to the generative AI technology

Details of the AI usage are given below:

- 1.
- 2.
- 3.

References

Ajraoui, Y. (2019). *Experimental characterization of electric motors and jet engines for blended wing body flight test models* [M. Sc Thesis]. Instituto Superior Tecnico, Lisboa, Portugal. 110p.

Cross, J. V., Walklate, P. J., Murray, R. A., & Richardson, G. M. (2003). Spray deposits and losses in different sized apple trees from an axial fan orchard sprayer: 3. Effects of air volumetric flow rate. *Crop Protection*, 22(2), 381–394. [https://doi.org/10.1016/S0261-2194\(02\)00192-8](https://doi.org/10.1016/S0261-2194(02)00192-8)

Dai, F. (2008). Selection and calculation of the blowing rate of air-assisted sprayers. *Plant Protection*, 34(6), 124–127. doi: 10.3969/j.issn.0529-1542.2008.06.032

Gu, C., Zou, W., Wang, X., Chen, L., & Zhai, C. (2022). Wind loss model for the thick canopies of orchard trees based on accurate variable spraying. *Frontiers in Plant Science*, 13:1010540. doi: 10.3389/fpls.2022.1010540

Gupta, P., Sirohi, N. P. S., & Mishra, I. M. (2012). Air flow characteristics of an air-assisted sprayer through horizontal crop canopy. *International Journal of Agricultural and Biological Engineering*, 5(1), 1–6.

Jin, Y., Qian, Y., Zhang, Y., & Zhuge, W. (2018). Modeling of ducted-fan and motor in an electric aircraft and a preliminary integrated design. *SAE International Journal of Aerospace*, 11(2), 115–126. <https://doi.org/10.4271/01-11-02-0007>

Jing, S., Ren, L., Zhang, Y., Han, X., Gao, A., Liu, B., & Song, Y. (2023). A simulation and experiment on the optimization design of an air outlet structure for an air-assisted sprayer. *Agriculture*, 13(12), 2277. <https://doi.org/10.3390/agriculture13122277>

Junaidin, B., & Cahyono, M. A. (2019). Conceptual design of Electrical Ducted Fan (EDF). *Prosiding Seminar Nasional Teknologi Informasi dan Kedirgantaraan: Peran Teknologi untuk*, Vol 5, pp 3-8. 10 December 2019. Yogyakarta. <https://doi.org/10.28989/senatik.v5i0.311>

Miao, Y., Chen, X., Gong, Y., Liu, D., Chen, J., Wang, G., & Zhang, X. (2023). Design and test of powerful air-assisted sprayer for high stalk crops. *Frontiers in Plant Science*, 14, 1266791. <https://doi.org/10.3389/fpls.2023.1266791>

Reichard, D.L., Fox, R. D., Brazee, R. D., & Hall, F. R. (1979). Air velocities delivered by orchard air sprayers. *Transactions of the ASAE*, 22(1), 69–80. doi:10.13031/2013.34968 69-80.

Ru, Y., Hu, C., Chen, X., Yang, F., Zhang, C., Li, J., & Fang, S. (2023). Droplet penetration model based on canopy porosity for spraying applications. *Agriculture*, 13(2), 339. <https://doi.org/10.3390/agriculture13020339>

Sharman, R. A. (2011). Electric ducted fan – theory and practice. RC Groups. com [on-line] Available: <https://www.rcgroups.com/forums/showatt.php?attachmentid=6384145>

Shi, R., Sun, H., Qiu, W., Lv, X., Ahmad, F., Gu, J., Yu, H., & Zhang, Z. (2022). Analysing airflow velocity in the canopy to improve droplet deposition for air-assisted spraying: a case study on pears. *Agronomy*, 12(10), 2424. <https://doi.org/10.3390/agronomy12102424>

Urban, D., Kusmirek, S., Socha, V., Hanakova, L., Hylmar, K., & Krau, J. (2023). Effect of electric ducted fans structural arrangement on their performance characteristics. *Applied Sciences*, 13(5), 2787. <https://doi.org/10.3390/app13052787>

van Rooij, N. E. (2019). *Analysis of a 3D printed Electric Ducted Fan for high-speed flight* [Master's Thesis]. Eindhoven University of Technology, 79p.

Wang, X., Feng, Y., Fu, W., Qi, J., & Song, J. (2023). Simple decision-making model for orchard air-assisted spraying airflow. *International Journal of Agricultural and Biological Engineering*, 16(2), 23–29. <https://doi.org/10.25165/j.ijabe.20231602.6849>

Wei, Z., Li, R., Xue, X., Sun, Y., Zhang, S., Li, Q., Chang, C., Zhang, Z., Sun, Y., & Dou, Q. (2023). Research status, methods and prospects of air-assisted spray technology. *Agronomy*, 13(5), 1407. <https://doi.org/10.3390/agronomy13051407>

Xue, X., Zeng, K., Li, N., Luo, Q., Ji, Y., Li, Z., Lyu, S., & Song, S. (2023). Parameters optimization and performance evaluation model of air-assisted electrostatic sprayer for citrus orchards. *Agriculture*, 13(8), 1498. <https://doi.org/10.3390/agriculture13081498>

Zhang, T., & Barakos, G. N. (2020). Review on ducted fans for compound rotorcraft. *The Aeronautical Journal*, 124(1277), 941–974. <https://doi.org/10.1017/aer.2019.164>

Zhao, Y., Tian, Y., & Wan, Z. (2022). Aerodynamic characteristics of a ducted fan hovering and transition in ground effect. *Aerospace*, 9(10), 572. <https://doi.org/10.3390/aerospace9100572>